Biomass Conversion and Biorefinery
https://doi.org/10.1007/s13399-022-03507-9

ORIGINAL ARTICLE

Multifunctional properties of silver and gold nanoparticles synthesis by *Fusarium pseudonygamai*

Mohamed K. Y. Soliman[1] · Mohammed Abu-Elghait[1] · Salem S. Salem[1] · Mohamed Salah Azab[1]

Received: 15 August 2022 / Revised: 25 October 2022 / Accepted: 27 October 2022

Abstract
The goal of the current work was to investigate the antibacterial, antibiofilm, anticancer, and antioxidant opportunities of silver and gold nanoparticles (AgNPs and AuNPs) synthesized utilizing a new fungus strain called *Fusarium pseudonygamai* TB-13c. With the aid of UV, HR-TEM, FTIR, SEM, and XRD, the NPs' creation was examined. For AgNPs and AuNPs, the mycosynthesized NPs' highest peak plasmon band was seen at around 420 and 540 nm, respectively. AgNPs ranged in size from 5 to 20 nm, whereas AuNPs ranged in size from 8 to 60 nm. AgNPs and AuNPs were spherical in form. For AgNPs, the angles were 38.42°, 44.56°, 64.66°, and 77.75°; for AuNPs, the angles were 38.56°, 44.74°, 64.87°, and 77.85°. The antibacterial efficiency of AgNPs and AuNPs was evaluated against *Klebsiella pneumoniae*, *Pseudomonas aeruginosa*, methicillin-sensitive *Staphylococcus aureus* (MSSA), and methicillin-resistant *Staphylococcus aureus* (MRSA). In particular, AgNPs outperformed AuNPs in their ability to combat pathogenic microorganisms. Furthermore, antibiofilm study that shown AuNPs had activity more than AgNPs. Interestingly, applying the DPPH procedure these noble metallic NPs had antioxidant activity, which the IC_{50} for AgNPs was 38.2 µg/ mL and 180 µg/ mL for AuNPs. The modification in the cells was evident in the cytotoxicity evaluation findings as change of their usual shape, partially or completely loss of monolayer, granulation, and shrinkage, or cell rounding with IC_{50} for normal vero cell were 695.34 µg/mL and 631.66 µg/mL for AgNPs and AuNPs, respectively, whilst IC_{50} for cancer cell (Mcf7) was 204.07 µg/mL for AgNPs and 206.95 µg/mL for AuNPs. The combined results show that there is a clear and flexible biological use for less toxic chemotherapeutic agents.

Keywords *Fusarium pseudonygamai* · Silver and gold nanoparticles · Antibacterial · Antibiofilm · Anticancer · Antioxidant activity

1 Introduction

Nanotechnology represents use of a tiny molecule with a unique size ranged from 1 to 100 nm [1–4]. Nowadays, nanotechnology is interfered in several applications as biological, pharmaceutical, photocatalysts, information technology, electrocatalysts, chemical science, physics, wastewater treatment, infection control, and cotton textiles [5–14]. Additionally, biotechnological applications, particularly those related to antibacterial, anticancer, biocompatibility, and anti-inflammatory properties, are growing. Three methodologies are available for generating nanoparticles [15–21]. Chemical, physical, and biological however the most recommended is green synthesize due to a lot of reasons as good defined size, clean, ecofriendly, cost-effective, safe, and shape nanoparticles synthesized [22–31]. The biological production of nanoparticles involves several types of living creatures, including plants, fungi, algae, bacteria, and viruses [32, 33]. However, fungi have more advantages due to fungal metabolites contain large number of proteins and enzymes which are highly effective in fabrication of nanoparticles, easily in downstream handling and scaling up, tolerance to metallic materials, economic facility, and production of huge biomass by several species of fungi [34–37]. There are many fungi has affinity to synthesize AgNPs and AuNPs extracellularly such as *Trichoderma saturnisporum*, *Phanerochaete chrysosporium*, *Fusarium oxysporum*, *Coriolus versicolor*,

✉ Salem S. Salem
salemsalahsalem@azhar.edu.eg

[1] Botany and Microbiology Department, Faculty of Science, AL-Azhar University, Nasr City, Cairo 11884, Egypt

Published online: 11 November 2022

and *Pleurotus sajorcaju* [38–41]. *Helminthosporium tetramera*, *Penicillium fellutanum*, *Schizophyllum radiatum*, and *Fusarium keratoplasticum* were rapidly produced silver nanoparticles [42–46]. Also, nano-sized gold particles produced by different species of *Fusarium oxysporum* and *Penicillium aurantiogriseumm* [47, 48]. In addition to, *Aspergillus sydowii* has ability to synthesize AuNPs from action of cell-free filtrate within a minute [49]. The most main problem that has a negative impact to the medical field is the infectious diseases that lead to the death of many people worldwide [50]. Nowadays, increasing resistance of microbes to traditional drugs is due to using antibiotics without lacking to the patients and generations of microorganisms with a development of virulence factors of pathogenic [51, 52]. Also, Au-NPs and Ag-NPs are highly displayed antibacterial properties for causative disease of Gram-negative bacteria as *Shigella dysenteriae*, *Pseudomonas aeruginosa*, *Enterobacter aerogenes*, *Klebsiella pneumonia*, *Salmonella typhimurium*, *Proteus mirabilis*, and, *E. coli.* Along with, Gram-positive pathogenic bacteria include *Enterococcus faecalis*, *Staphylococcus epidermidis*, *Bacillus subtilis*, *Staphylococcus aureus*, and *Streptococcus pyogenes* [53–57]. Moreover, bacteria have been developed additional strategies, including biofilm formation, to evade the actions of many inhibitors. Biofilms are abiotic or biotic substances which are a community of living microorganisms that establish a strong connection between them and the surface that are connected [58, 59]. This connection is mediated by substances secreted by microorganisms present in the biofilm [60, 61]. Additionally, the presence of biofilm matrix around the bacterial cells is the other reason to resistance of bacteria to well-known antimicrobial agents. So, non-traditional antibiotics have a great interest by many researchers to in resolve this challenge by production of novel nano antibiotics compound which can be overcoming resistant of pathogenic microorganisms [62, 63]. Furthermore, medical transplantation has a bad effect due to presence of bacterial, so sterilization and uses of materials have antibiofilm activity are some ways to limit formation of biofilm [64]. Furthermore, the common components interfere in the composition of biofilm are extracellular polymeric molecules as proteins, polysaccharides, and extracellular DNA [65]. Additionally, bacterial biofilms indicate a possible alteration in its structure and function when exposed to biomolecules [58]. Obviously, development of a novel compounds has ability to destroy and prevent bacterial biofilm through a recent mode of action is the resolving of these problems [66–68]. Cancer seems to be nowadays the second major incidence of dying in developed nations, giving it a severe health issue. It is a multi-step process that is defined by aberrant cell proliferation and is brought on by alterations in the genetic makeup and modified by environmental variables [69]. There are many different cancer medicines in use today, and significant improvements are continually being studied. Nanotechnology has just come to light as a reasonable alternative for a number of challenges, and it has been thought to bring about a fundamental alteration in the identification, management, and therapy of malignancy [70].

In the current work, AgNPs and AuNPs were mycosynthiezed using *Fusarium pseudonygamai*, as well as their nanostructures were characterized by several analyses. Moreover, this study aimed to assess mycosynthesized AuNPs and AuNPs in various biomedical applications including antimicrobial, antibiofilm, anticancer, and antioxidant efficacies.

2 Materials and methods

2.1 Materials

Silver nitrate ($AgNO_3$) and chloroauric acid ($HAuCl_4$) were purchased from Sigma-Aldrich, USA, for chemicals and used as precursors for preparation Ag-NPs and Au-NPs. Other chemicals, culture media, and reagents used in this study were purchased from Modern Lab Co., India, in analytical grade without any purification required.

2.2 Isolation and identification of fungal isolates

From several agricultural soil sites in Qalyub, Egypt, 15 soil samples have been taken. After successive dilutions of the soil samples, the inoculum was plated on potato dextrose agar (PDA) and incubated at 28 ± 2 °C for 3–4 days to isolate the fungi. Chloramphenicol (10 µg/mL) added to the medium after autoclaving assisted in preventing bacterial contamination. Purity of the fungal growth was evaluated, and the isolated fungus was injected in the cultural slant for conservation at 4 °C for additional investigation. Molecular identification using genomic DNA as well as its region amplification, first most efficient fungal strain, was genetically identified. For the ITS-based sequencing, 0.1 g of fungal mycelium genomic DNA was extracted. The Gene Jet Plant genomic DNA purification Kit (Thermo) #k0791 procedure has been used to extract the DNA. ITS1 and ITS4 have been the primers employed. The Maxima Hot Start PCR Master Mix (Thermo) #k0221 by Sigma Scientific Services Company (Cairo, Egypt) was used in the following amplification (PCR) procedure: Thermo's Maxima Hot Start PCR Master Mix, 0.5 µM from each primer, as well as 1 µL of isolated fungal genomic DNA, were all added to a 50 µL PCR mixture. In a DNA Engine Thermal Cycler, the PCR was carried out with a hot start at 94 °C for 3 min, followed by 30 cycles of 94 °C for 30 s, 55 °C for 30 s, and 72 °C for approximately 60 s, then a further 10 min at 74 °C of extension. Using forward and reverse primers and an ABI 3730 1 DNA sequencer, the specimens subsequently processed by GATC Company (Germany).

2.3 Screening of biosynthesis AgNPs and AuNPs using fungal isolates

On an orbital shaker, 1 mM of silver nitrate ($AgNO_3$) was combined with cell-free filtrate and incubated at 28 ± 2 °C for 24 h (120 rpm). After the incubation period was through, the color change could be seen for up to 72 h. After that, the samples were separated and dried at 150 °C for 48 h. Eventually, the bio-transformed product was collected and submitted for more investigation. The same procedures for chloroauric acid ($HAuCl_4$) were used to create gold nanoparticles instead of silver nitrate.

2.4 Biosynthesize of AgNPs and AuNPs by fungal isolate TB-13c

Fungal isolate TB-13c was cultivated for three days at pH 6.0, 28 ± 2 °C, and 140 rpm shaking inside a 250-mL flask that contain 100 mL of Czapek Dox (CD) broth medium. Then, fungal biomass subsequently was filtered and rinsed repeatedly by sterile D H_2O water to eliminate any medium constituents. The resulting suspension of the fungal biomass in sterile distilled water (1:10) was then agitated for couple of days at 28 °C at 150 rpm, whilst also collecting the fungal biomass using filter paper. The synthesis of AgNPs and AuNPs utilized the cell-free filtrate in the manner described below. Before incubating with cell-free filtrate at 28 ± 2 °C for 72 h on an orbital shaker (150 rpm) in the dark, 1 mM of $AgNO_3$ and $HAuCl_4$ were combined, and the pH was then adjusted at 10 for AgNPs and 5 for AuNPs. Following the incubation time, AgNPs and AuNPs showed a brown and violet colors, respectively. The latter was separated and dried for 48 h at 150 °C. Eventually, the bio-transformed product was gathered and submitted for more research.

2.5 Characterization of AgNPs and AuNPs

AgNP and AuNP biosynthesis were detected using to detect an intense absorption peak associated with surface plasmon excitation, to acquire the optical UV–Vis absorption properties, use the JASCO 730 double beam spectrophotometer at wavelengths 200–700 nm. AgNPs and AuNPs that were synthesized from biological materials were measured using a transmission electronic microscope (TEM) (JEOL-2100). In order to achieve this, standard copper grids being given a drop of NP-containing solution to apply, which was followed by a full night of vacuum drying before the grids were put into a specimen container. Additionally, using Fourier transform infrared (FTIR) spectroscopy (JASCO, FT/IR- 6100), several functional groups found in biofabricated NPs molecules were examined. AgNP and AuNP samples were blended with KBr before being crushed firmly into discs. To get FTIR spectra, these discs were scanned between 400 and 4000 cm^{-1}. The morphological properties and constituent structures of mycosynthesized AgNPs and AuNPs were examined using SEM coupled to a JEOL JSM-6510 LV energy-dispersive spectroscope (EDS) instrument. The crystal structures of silver and gold NPs were described by XRD analysis (XRD, X PERT PRO-PAN Analytical).

2.6 Antimicrobial activity

The MIC values of two different substances (AgNPs and AuNPs) were examined against a multidrug resistant strains (MRSA, MSSA, *P. aeruginosa*, and *K. pneumonia*) using the broth microdilution technique. AgNPs and AuNPs were prepared at various concentrations (1000, 500, 250, 125, 62.5, 31.25, and 15.75 µg/mL). Test samples (100 µL) of various concentrations were added to 100 µL of double-strength Mueller Hinton (MH) broth-filled sterile microtiter plate wells. In all wells save the negative control one, bacterial cell suspension (20 µL) corresponding to (OD comparable to 0.5 McFarland standard) was administered. To test whether MH broth could adequately support bacterial growth, bacterial solution was added to positive control wells. The MH broth and sterile distilled water used in the negative control wells were used to ensure sterility. The plates were incubated for 24 h at 37 °C. After that, the plate subsequently re-incubated again for 6 h with 30 µL of resazurin solution (0.02 percent wt/v) (HiMedia) added to each well to detect bacterial growth. Bacterial growth was indicated by a shift in color from blue to red. Growing the strains properly was shown by a change in the color of the growth control wells to red, and the absence of contamination was indicated by no change in the color of a sterile control well. The experiment is performed three times, and mean values were reported.

2.7 Biofilm inhibition in vitro

With minor modifications, the microtiter plate (MTP) approach was used to assess the capacity of AgNPs and AuNPs to prevent or lessen the aggregation of biofilms in clinical species *S. aureus* and *Pseudomonas aeruginosa* (recognized as a prolific biofilm-producing strain) [71]. In a nutshell, tryptic soy broth media (TSB) with 1% glucose was added on a flat-bottomed MTP along with gradient concentrations of AgNPs and AuNPs. Test organisms were cultured overnight using a 1:100 dilution to achieve an inoculum size of 1.5 108 CFU/mL, which was subsequently loaded onto MTP and incubated at 37 °C for 48 h. In order to evaluate growth density, spectrophotometry was used (O.D. 620 nm), and following that, planktonic cells were removed from all of the MTP wells without causing any damage to the biofilm that had already grown. Furthermore, to remove the residue cells of floated unbounded cells, these wells were washed by

phosphate-buffered saline (PBS) at pH 7.4, three times. For fixation of biofilm, methanol 95% was added in equal volume 200 µL to all wells. After that, 200 µL of 0.3% crystal violet (CV 0.3%) was added to the same wells, then incubation of the plates at 20–25 °C for 15 min. Additionally, the excess of CV stain was gently removed by sterile distilled H_2O. Lastly, CV stain bounded with biofilm, at this point was examined then photographed using an inverted microscope (Olympus Ck40) × 150. Adding 200 µL of 30% acetic acid to each well allowed for the quantitative measurement of biofilm development, and the microplate reader (Tecan Elx800) was used to measure the color at 540 nm. Results from treated and untreated wells were contrasted.

2.8 Anti-oxidant activity

2.8.1 DPPH screening

The DPPH (2, 2-diphenyl-1-picrylhydrazyl) technique was used to test the antioxidant capacity of AgNPs as well as AuNPs [72]. The amounts of DPPH radicals that were scavenged at various nanoparticle concentrations (1000 µg/mL, 500 µg/mL, 250 µg/mL, 125 µg/mL, 62.5 µg/mL, 31.25 µg/mL, and 15.62 µg/mL) were measured. Antioxidant activity of standard and NPs was determined as DPPH scavenging activity (%): [((control absorbance − extract absorbance)/(control absorbance)) × 100].

2.9 Cytotoxicity and anticancer potential

2.9.1 Cell culture

The human mammary gland, breast, produced from a metastatic location, normal Vero cells (kidney of an African green monkey), and cancer cells (Mcf7-HTB-222) were purchased from ATCC.

2.9.2 MTT assay

A full monolayer sheet formed after 24 h of incubation at 37 °C with 1 × 105 cells/ml (100 µL) in the 96-well tissue culture plate. After a confluent sheet of cells had grown, the 96-well microtiter plates' growth material was decanted, and the cell monolayer had been twice rinsed with washing media. In RPMI medium containing % serum, two-fold serial dilution of the sample was created (maintenance medium). Three wells served as the control wells and received just maintenance medium, while 0.1 ml of each dilution was tested in various wells. The plate was tested after 37 °C of incubation. The physical characteristics of cytotoxicity, such as problems such as loss of the monolayer, rounded, shrinking, or cellular granulation, were examined in the cells (5 mg/mL in PBS) of MTT solution has been created (BIO BASIC CANADA INC). To every well, 20 µL of the MTT solution was then added. To completely blend the MTT through into medium, put on a shaker and shake for five minutes at 150 rpm. Permit the MTT to metabolize for four hours in an incubator (37 ºC, 5% CO_2). Get rid of the media (if required, dry plate on paper towels to get rid of any leftovers. In 200 µL of DMSO, resuspension of formazan (MTT metabolic product). For 5 min, shake at 150 rpm to properly combine the formazan and solvent. At 620 nm, remove background when reading optical density. Cell number and optical density ought to be closely connected [73].

3 Results and discussion

3.1 Screening of various soil fungi for biosynthesis of AgNPs and AuNPs

The most potent microorganism in the soil is fungi, which have a good potential for biofabriacted of metallic nanoparticles. The aim of our study is the isolation of different soil fungi species for mycosynthesize of silver and gold nanoparticles. In addition, this study aimed to evaluate both AgNPs and AuNPs in various biological activities including antimicrobial, antibiofilm, anticancer, and antioxidant efficacies. Among which, 15 soil samples were collected from various site in Qalyub governorate, Egypt. All the samples of soil were cultivated on Potatoes Dextrose Agar (PDA) medium, 30 individual fungal strains were isolated. Furthermore, screening for the capability of 30 isolates for synthesize of AgNPs and AuNPs were applied. Of them, 11 isolates showed positive synthesize for both nanoparticles; 5 of these species did so in less than eight hours. In addition, only 11 isolates produced AgNPs and only one species produced AuNPs. Out of the 14 species of *Aspergillus* that were continuously studied, 5 species continuously generated extracellular AgNPs and AuNPs, 5 isolates only produced AgNPs, and 1 species created gold NPs. Followed by *Fusarium* species, out of 6 strains tested, 4 have a better response for the mycosynthesis of AuNPs and/ or AgNPs, and alone one strain mycosynthesized AgNPs. Of the 4 species screened, 2 species of *Penicillium* have synthesized AgNPs and one biofabriacted the two nanoparticles. Three *Trichoderma* species was the two strains had been synthesized AgNPs and one with strong synthesize both of AgNPs and AuNPs. AgNPs did synthesize by one *Mucor* isolates from two isolated. Finally, the only species of *Rhizopus* was isolated not give any response to both metal nanoparticles. In current study, only one fungal isolate (TB-13c) showed

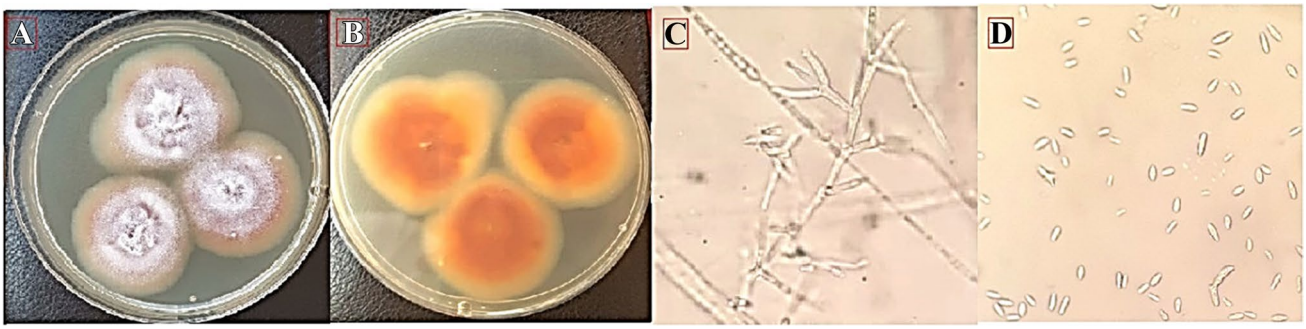

Fig. 1 Morphological identification of *Fusarium pseudonygamai* TB-13c: **A** growth area on PDA; **B** colony opposite color; **C** and **D** conidiophore and conidia under optical microscope, respectively

high potency to produce AgNPs and AuNPs. During this whole study, *Fusarium* spp. (TB-13c) was identified as suitable strains for the extracellular fabrication of metallic nanoparticles depending on the particles durability and quicker rate of production (Fig. 1). Similar to this, several studies have used *Fusarium* spp. as prospective candidates for the formation of either silver or gold nanoparticles [41, 47, 74].

Molecular techniques were used to identify the fungal isolate *Fusarium pseudonygamai* TB-13c. Using PCR as well as sequential methods, the ITS segment of a filamentous fungi was discovered. We created a phylogenetic tree utilizing something such as a greatest probability approach to compare our ITS sequence to earlier identified sequences. According to Fig. 2, the outcomes demonstrated a 100% agreement between the sequenced ITS segment and the structure of *Fusarium pseudonygamai* TB-13c.

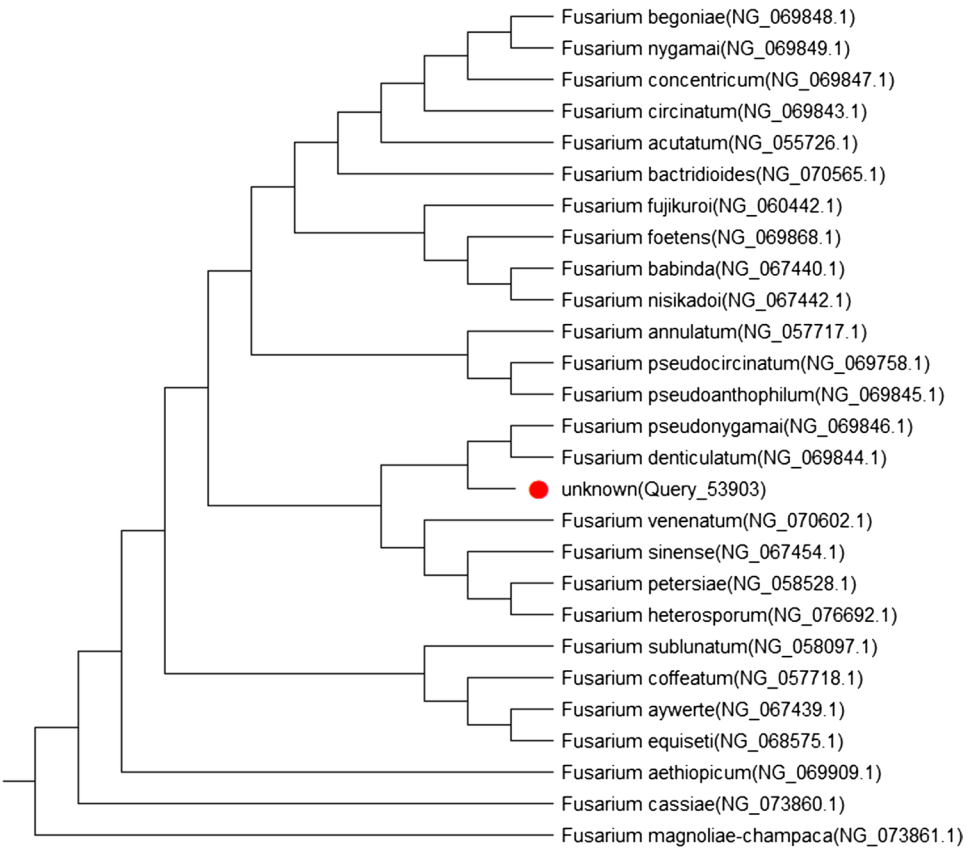

Fig. 2 Phylogenetic tree incorporating the fungal strain TB-13c ITS sequences matching NCBI sequences, identified as *Fusarium pseudonygamai*

3.2 Characterization of AgNPs and AuNPs

As NPs develop, their colors change, becoming brown for AgNPs and pinkish violet for AuNPs, respectively. UV–vis range significantly supports its manufacturing. Absorbance spectroscopy mostly in UV–vis spectrum, from 300 to nm wavelength, is referred to as UV–vis spectroscopy. This method is important when figuring out how NPs develop, aggregate, and remain stable. Noble nanoparticle such gold and silver have higher absorption wavelengths (max) that are between 500–550 nm and 400–450 nm, respectively. Consequently, we could verify that perhaps the correct NPs have indeed been generated whenever we notice the highest value in particular wavelength areas. There is a chance that NP will aggregate over time, which would also cause max to adjust more towards the relatively long wavelength range. The production of these AgNPs and AuNPs were primarily verified by UV–vis spectroscopy, with maximal assimilation occurring at 420 and 540 nm, respectively (Fig. 3).

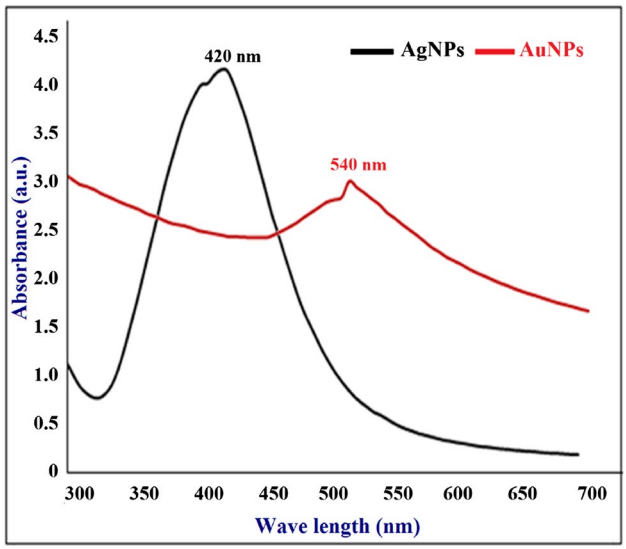

Fig. 3 UV–vis spectrophotometer of the mycosynthesized AgNPs and AuNPs

TEM examination is the most efficient method for determining the morphological characteristics of mycosynthesized NPs, such as their shape and size. In Fig. 4A TEM image displayed well-distributed, almost spherical AgNPs, and in the center right corner displayed the SAED structure. AgNPs exhibited a particle size range of 5–20 nm, as seen in Fig. 4B. In contrast, AuNPs were spherical and 8–60 nm in size (Fig. 4C). Interestingly, the SAED pattern

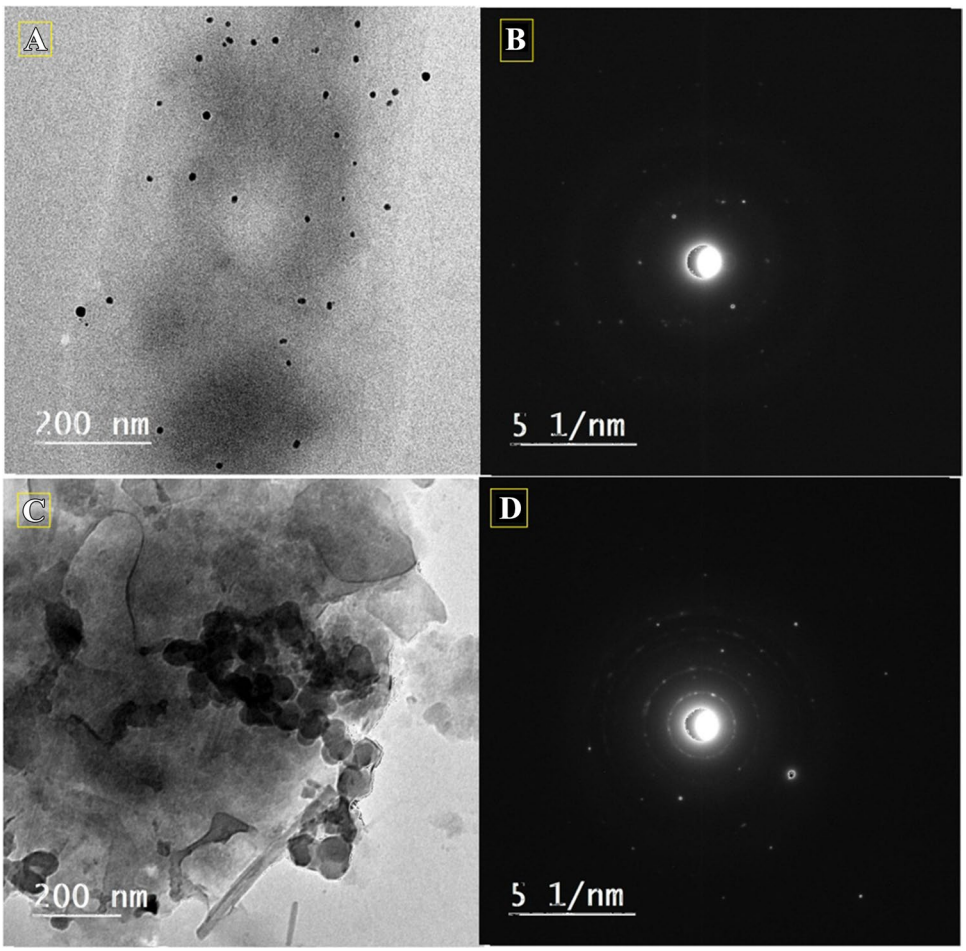

Fig. 4 **A** TEM image of AgNPs, **B** SAED patterns of AgNPs, **C** TEM image of AuNPs, and **D** SAED patterns of AuNPs

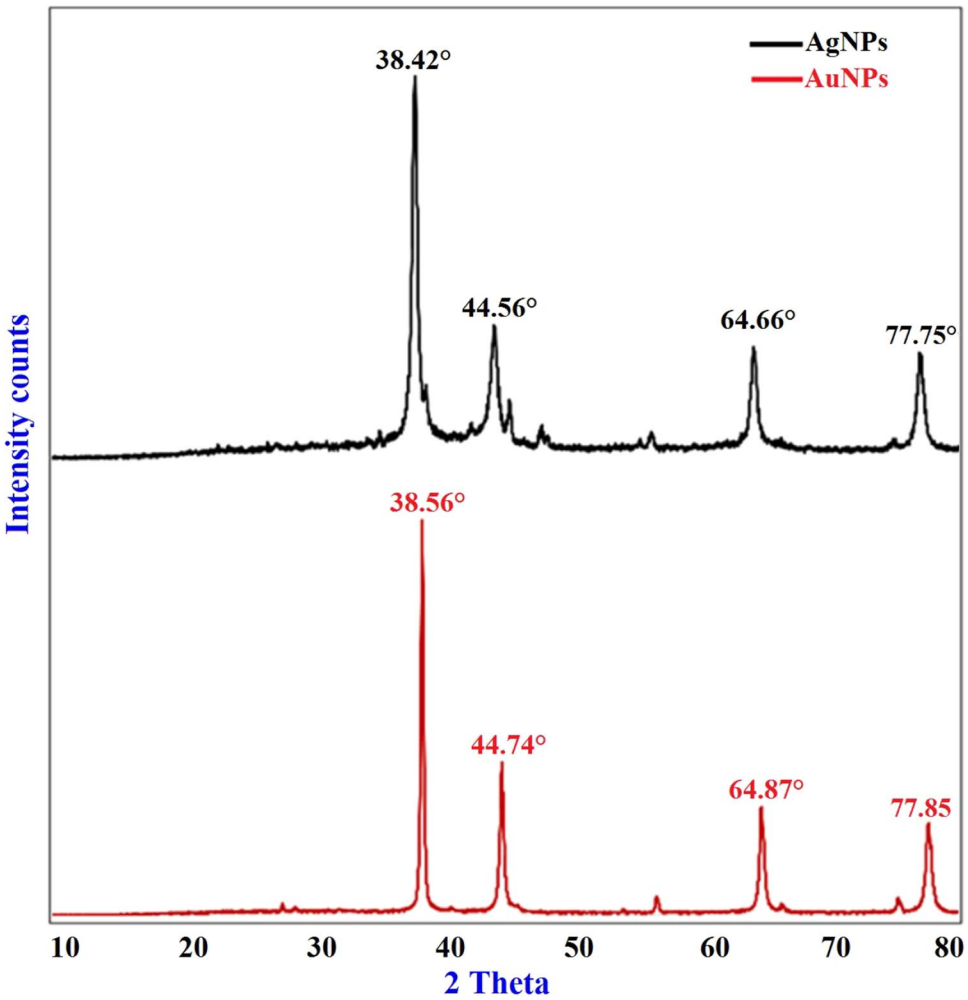

Fig. 5 XRD pattern of AgNPs and AuNPs biosynthesized by *Fusarium pseudonygamai*

of AuNPs was also seen in Fig. 4D. The myco-fabricated NPs matched those from earlier research in regards to size and form [38, 40].

Figure 5 shows the XRD patterns of AgNPs and AuNPs. Four different diffraction peaks may be seen in each spectrum. Peaks are seen in the case of AgNPs at four values: 38.42°, 44.56°, 64.66°, and 77.75°. Peaks throughout AuNPs were shown at 2θ values: 38.56°, 44.74°, 64.87°, and 77.85°. These 4 peaks correspond to reflections from of the planes (111), (200), (220), and (311) of a face-centered cubic phase of AgNPs and AuNPs. The peak matching to the (111) plane is much stronger in both situations than the peaks belonging to the (200), (220), and (311) planes. This suggests that the nanoparticles may be predominantly oriented all along (111) planes. Consequently, the XRD investigation obviously demonstrates that the produced AgNPs and AuNPs are crystalline. These findings are consistent with previous research [75, 76].

In the research lab, substances can be examined using FT-IR. The absorbance peaks in an infrared spectrum, primarily reflect on the vibrational frequencies between both the atomic bonds of the specimen undergoing examination, serve as the sample's fingerprint. Due to the unique atomic bonds that each substance has, no two compounds with the same infrared spectrum are exactly comparable. As a result, infrared spectroscopy can be useful for qualitative investigation and improved identification of various materials. The peak sizes also fall within the range that reveals the quantity of substance present. Advanced software algorithms make this spectroscopy a great tool for quantitative analysis [77]. The metal–oxygen resonance is responsible for the peaks inside the area between 400 and 700 cm^{-1} of the FT-IR spectrum seen in Fig. 6. In this study, the formation of silver nanoparticles can be confirmed by the presence of a peaks at 510, 620 and 832 cm^{-1} belong to bending vibration of Ag–O. The occurrence of those same peaks with a little

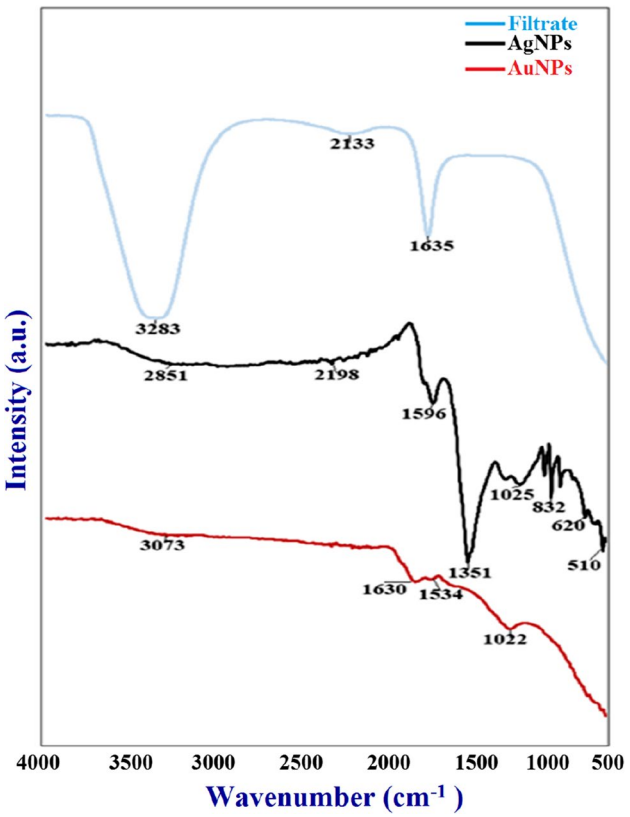

Fig. 6 FTIR spectra of fungal filtrate, AgNPs and AuNPs biosynthesized by *Fusarium pseudonygamai*

variance in the wavenumber has previously been described [78–80]. FT-IR analysis has been used to investigate the existence of secondary metabolites that cap and reduce silver nitrate precursor to AgNPs. The occurrence of several functional groups in *Fusarium pseudonygamai* extract was correlated with the presence of various IR bands. In this study, the IR spectra investigated for the silver nanoparticles revealed the absorption peaks at (I) 2851 and 2198 cm^{-1} (OH group of alcohols and phenols); (II) 1596 cm^{-1} and 1351 cm^{-1} (C = O stretching of carboxylic acid group); (IV) 1025 cm^{-1} (C–OH vibrations of the protein/polysaccharide). Additionally, Ag–O was assigned the characteristic bands at 832,620, and 510 cm^{-1}. The above peaks were confirmed in the previous studies [81, 82]. Additionally, the O–H stretching vibration of the hydroxyl groups in alcohol and phenol is seen in the FTIR spectra of AuNPs with what appears to be a unique band at wavenumber 3073 cm^{-1}. The band at 1630 cm^{-1} is due to asymmetric CH_2 stretching. The band at 1534 cm^{-1} display aromatic rings. The aromatic ring and OH assignments do certainly imply the polyphenolic attachment towards the gold surface. Furthermore, the distinctive band for Au-O was designated at 1022 cm^{-1}. It follows that the various metabolites present in the filtrate of the fungal strain play a major part in the production and size reduction of Ag and Au into a well-stabilized nano-form.

SEM image confirmed the existence of nanoparticles ranging in size from 10 to 61 nm for AgNPs as shown in Fig. 7A. The existence of metal Ag and Au was substantiated by EDX spectrum analysis, which exhibited peaks within their typical energy levels. The identification lines presented for the principal emission energies for Ag correlate to the peaks observed in the spectrum, providing confidence that Ag was accurately characterized wherein the peak situated approximately 3 and 4 keV (Fig. 7B). The nanoparticles revealed that spherical AuNPs with sizes ranging from 15 to 70 nm (Fig. 7C). Those maxima are directly related to the Ag characteristic. Similarly, an absorption peak obtained at ~2 keV which is specifically related to characteristic of AuNPs obtained in the spectrum (Fig. 7D). The mass of Ag was 23.76% with atom of 6.18%, whereas for gold, it is 61.97% with atom of 10.17%. The Au-NPs and Ag-NPs were discovered to really be crystalline exhibiting oval as well as spherical shapes, correspondingly. SEM examination normally provides an in-depth picture resolution of something like the particles by assigning a focused beam of electrons over the surface and finding secondary or backscattered electron signal. In comparison, EDX also was utilized to offer atomic identification and concentration profiles information. SEM–EDX was used to investigate the surface analysis, topology, structural organization, and energy dissemination of biologically synthesized nanoparticles in our work. Previous research found polydisperse AgNPs acquired with high-resolution pictures, indicating excellent crystallinity of the nanoparticles and a strong signal in the Ag area, verifying the production of AgNPs [83]. These study have established that metallic Ag nanocrystals have a characteristic optical maximum absorption about 3 keV cause considerable plasmon resonance.

3.3 Minimum inhibitory concentration of AgNPs and AuNPs

The actions of AgNPs and AuNPs against harmful microorganisms are among their major benefits. As a result, the antibacterial effectiveness of mycosynthesized both AuNPs and AgNPs against pathogenic Gram-positive (MRSA and MSSA) and Gram-negative (*P. aeruginosa* and *K. pneumonia*) bacteria was initially examined. Inhibitory effects of various doses of AgNPs and AuNPs (15.62–1000 µg/ mL) were studied (Fig. 8). The results indicated that the MIC for AgNPs was 62.5 µg/ mL against MSSA, *K. pneumoniae*,

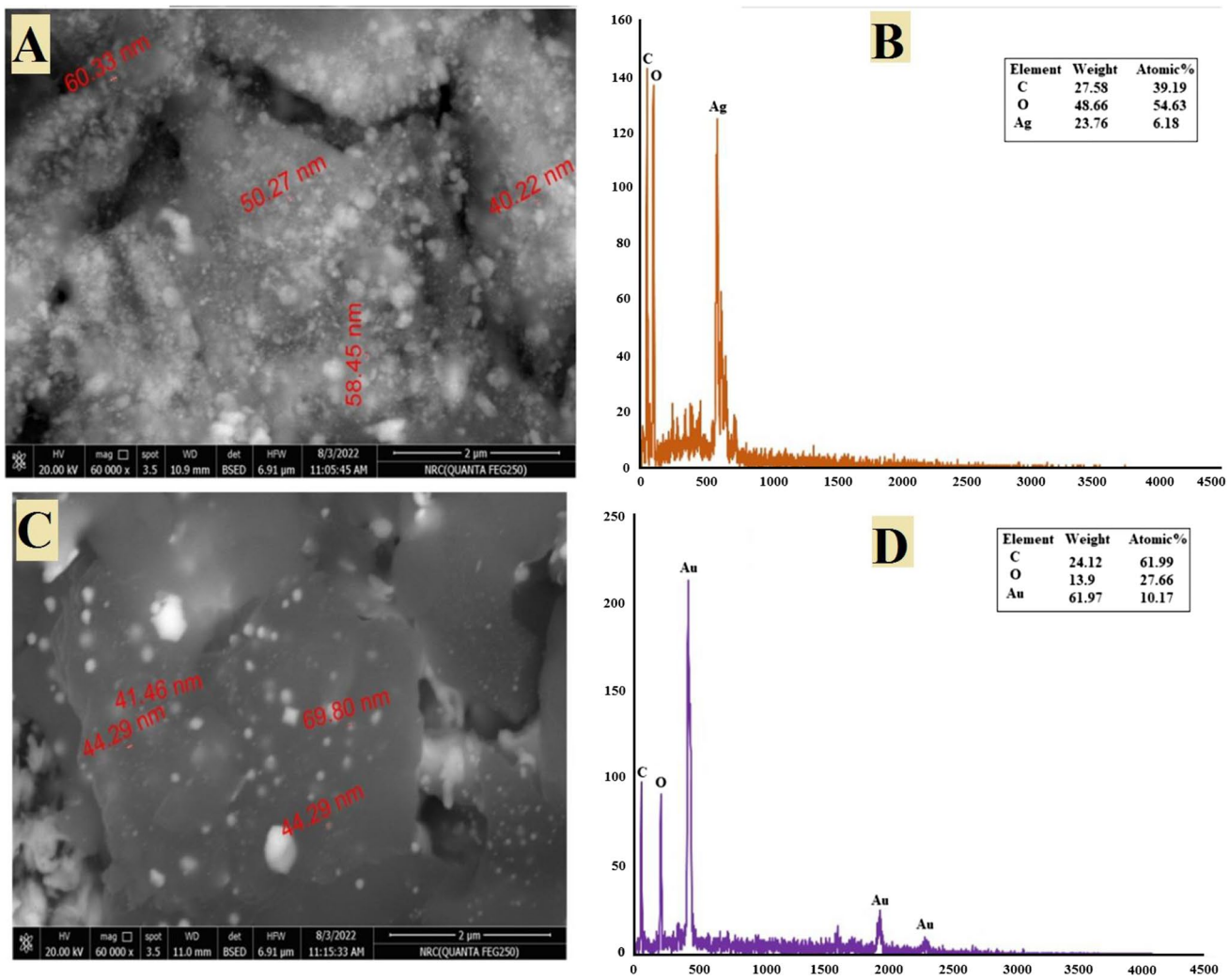

Fig. 7 SEM–EDX spectrum of mycosynthesize AgNPs (**A** and **B**) and SEM–EDX spectrum of mycosynthesize AuNPs (**C** and **D**)

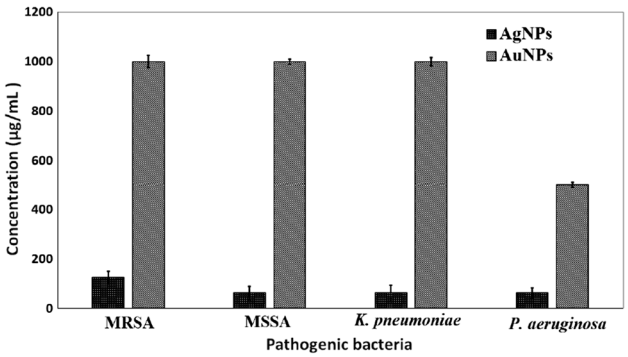

Fig. 8 Antibacterial activity of AgNPs and AuNPs against different pathogenic bacteria

and *P. aeruginosa* and 125 g/ mL against MRSA, whereas the MIC for AuNPs was 1000 µg/mL versus MRSA, MSSA, and *K. pneumoniae* and 500 µg/mL for *P. aeruginosa*. Additionally, AgNPs outperformed AuNPs in their ability to combat both Gram-positive as well as Gram-negative harmful microorganisms. According to another study, nanoparticles inhibit bacterial growth by binding with phosphorous moieties in DNA. This inhibits DNA replication, which lowers enzyme activity [84]. Additionally, it can prevent the generation of ATP, which results in cell death, and block the respiratory enzymes of bacterial cells. Additional alterations included membrane detachment, cytoplasmic shrinkage, and finally membrane of cell rupture [85, 86].

3.4 Anti-biofilm of AgNPs and AuNPs

The antibiofilm efficacy of nanoparticles in this study shown variable effects against various bacteria. Accordingly, when used at concentrations below the MIC value, AuNPs showed the greatest efficacy against the development of biofilms caused by *S. aureus* and *P. aeruginosa*.

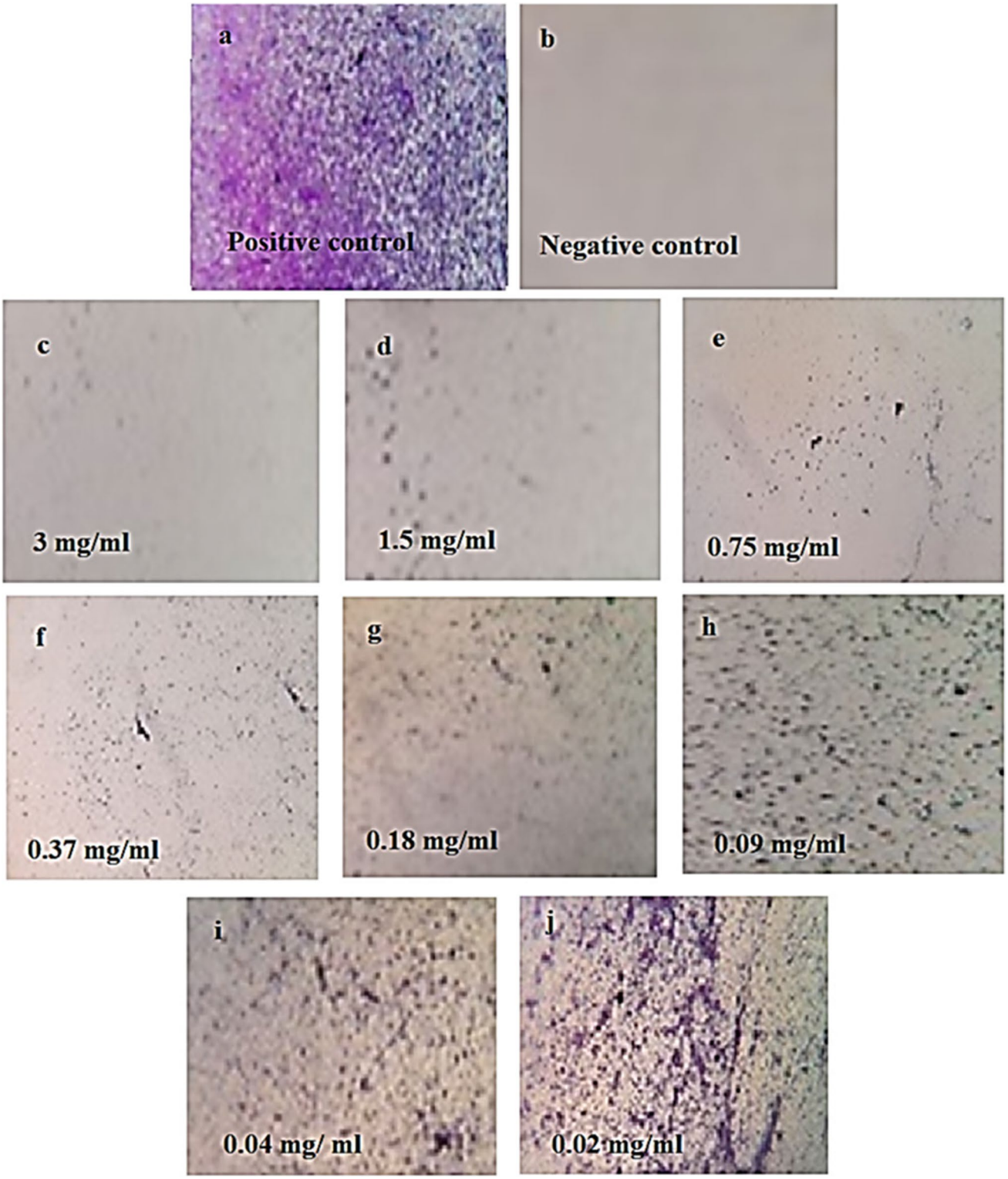

Fig. 9 Light inverted microscopic images of *S. aureus* biofilm grown with various concentrations of AuNPs: **a** 0.0 mg/mL represents the positive control; **b** negative control; **c**, **d**, and **e** 3.0 and 2.0 µg/mL above the MIC value; **e** 0.5 µg/mL; **f** 0.125 µg/mL; 0. 062 µg/mL; **h** 0. 031; **i** 0.04 µg/mL; and **j** 0.02 µg/mL. At concentrations from 0.04 and 0.02 µg/mL, (**i** and **j**) bacteria have manifested as dispersed cells and are unable to assemble to form a typical biofilm

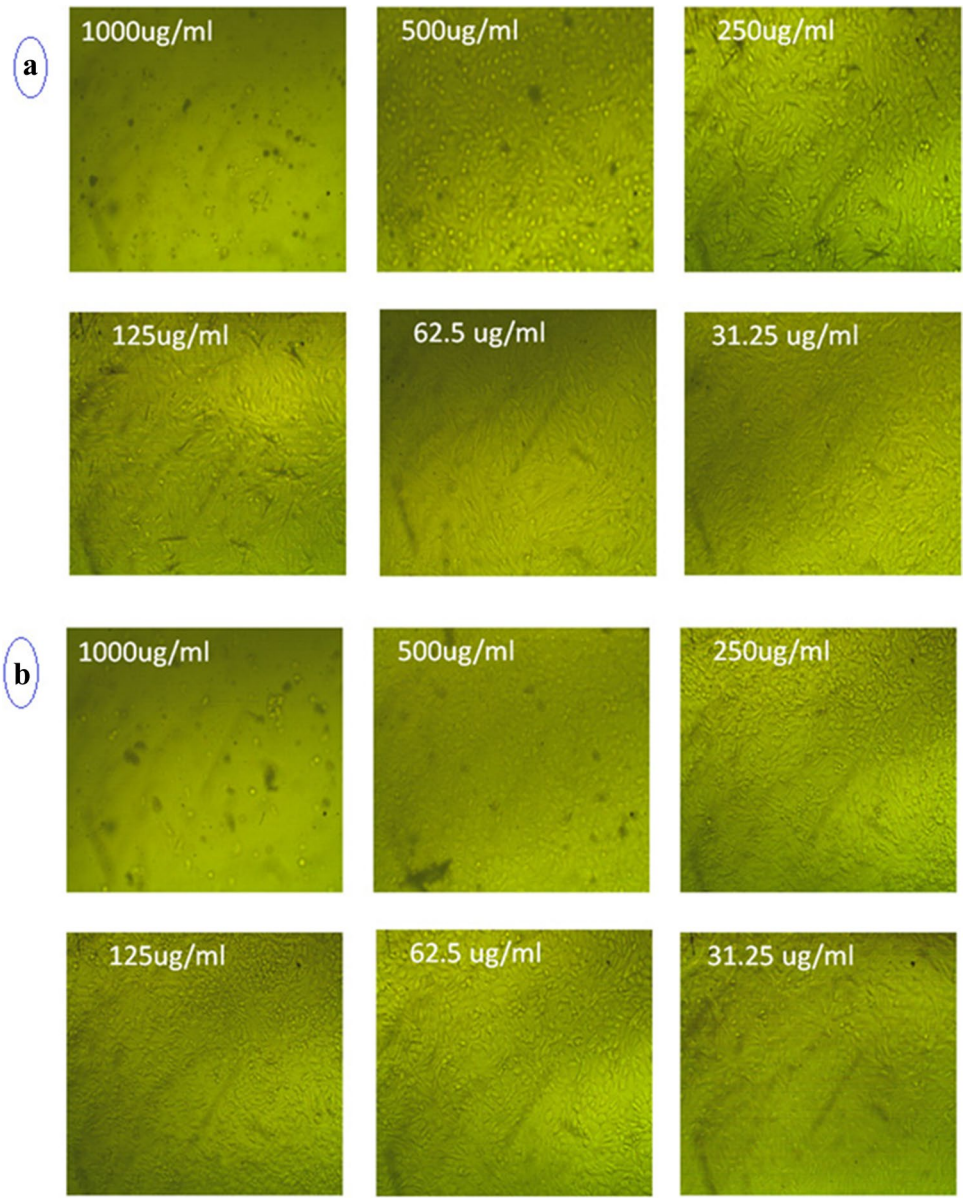

Fig. 10 Effect of AgNPs (**a**) and AuNPs (**b**) on normal Vero cells at different concentration imaged by light inverted microscope

Against *P. aeruginosa*, AuNPs at 250, 125, 62.5, 31.25, and 15.62 µg/mL decreased the production of biofilm by 89.24, 87.28, 86.3, 78.97, and 78.48%, respectively. Additionally, at concentrations below the lethal dosage without impairing bacterial growth, Au-NPs demonstrated significant biofilm prevention agent against *S. aureus*, with proportions of 92.9, 75.6, 75.1, 67.3, and 63.8%, respectively. Through inverted microscopy techniques, the impact of nanoparticles on the surface structure of the biofilm matrix was investigated. The results showed that the positive control sample had a biofilm matrix, while Au-NPs-treated wells showed less surface colonization and biofilm matrix in *S. aureus*. By dissolving the micro-colonies inside the specimen that was permitted to be treated in the range of 3000 to 0.02 µg/mL, the light microscopic images showed that the AuNPs had completely dispersed the biofilm Fig. 9. According to their respective quantitative and qualitative analyses, AuNPs reduced the growth of both *S. aureus* as well as *P. aeruginosa* biofilms during the initial stage. In contrast, AgNPs had a little inhibited effect against *P. aeruginosa* and *S. aureus* which inhibited up to 43.7% at 15.6 µg/mL, and 41.3% at 7.8 µg/mL for *P. aeruginosa* and no inhibition against *S. aureus* under MIC value. Another study found that AuNPs produced also with fungal strain *Laccaria fraterna* reduced biofilm growth in almost the same way. Our results were likewise phenotypically like that of Rajkumari et al. [87]. Utilizing Baicalin conjugated nanoparticles, they contributed to a reduction biofilm forming capability. The results of our crystal violet technique for biofilm inhibition corresponded to those of Khan et al. [88]. Past study by Estevez et al. showed that

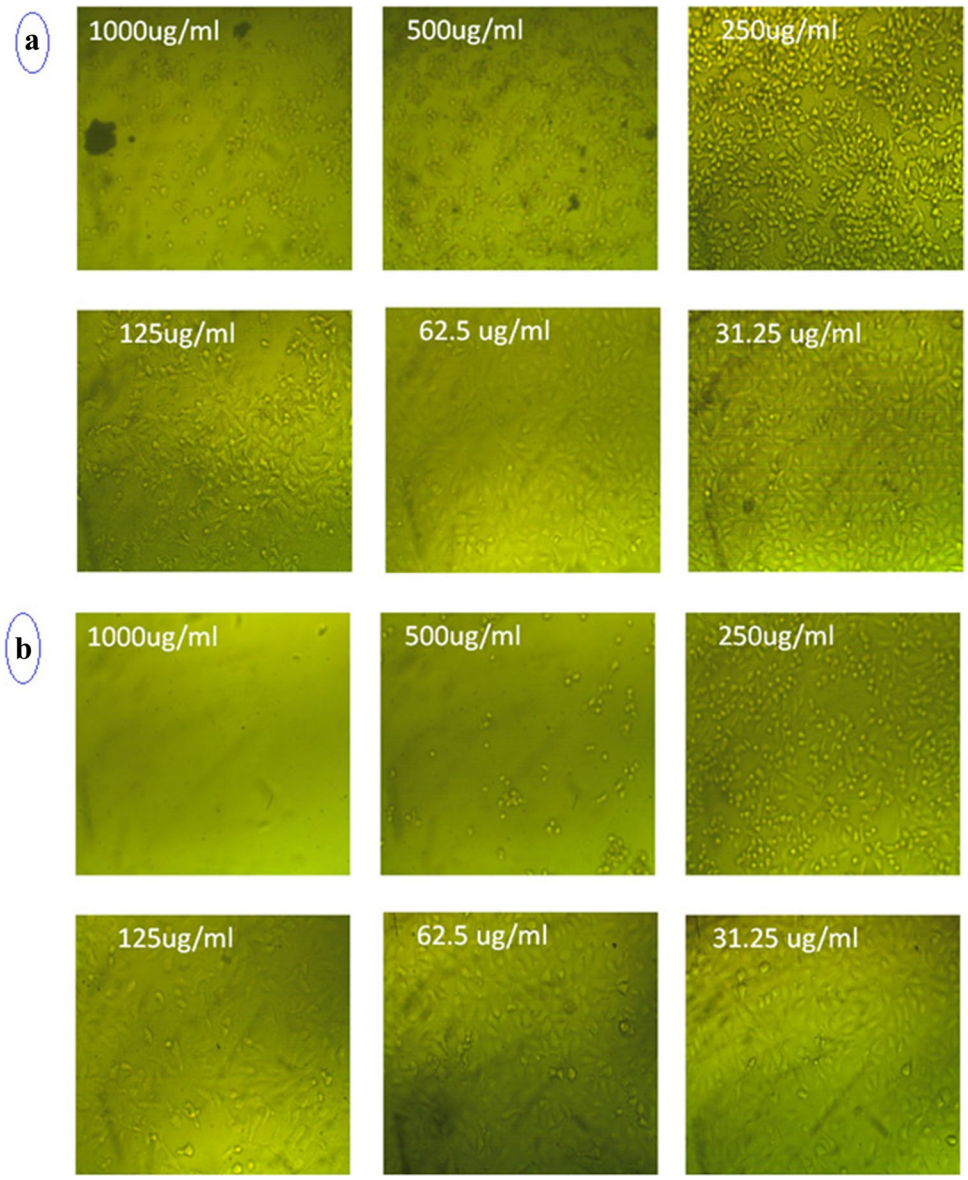

Fig. 11 Effect of AgNPs (**a**) and AuNPs (**b**) on cancer cells (Mcf7) at different concentration imaged by light inverted microscope

AgNPs can diffuse into the matrix and damaged cells in the biofilm's intern al layer [89].

3.5 Cytotoxicity of AgNPs and AuNPs

The shape of cells the first and most noticeable finding arising from exposure to nanoparticles or other toxic compounds is a change in cell shape and otherwise morphology of the cell in culture. As a result, the light inverted microscope may be developed to monitor damage to cellular shape and morphology as a result of AgNPs and AuNPs exposed dosage (Figs. 10 and 11). The normal cell line expanded continuously across the plates and displayed epithelial shape. Cells after treatment to various concentration of AgNPs or AuNPs eventually lost unique phenotypic characteristics. Additionally, at high concentrations of AgNPs and AuNPs, the cells exhibit full or partial breakdown of monolayer, cell granulation, rounding, or shrinkage as compared to control sample. The light inverted microscope picture demonstrated unequivocally that the damage induced in cell morphology is dosage dependent for AgNPs and AuNPs.

3.6 MTT assay

The fundamental step in toxicology which explains the cellular reaction to a toxin is called a viability test. They often provide details on cell metabolism, cell growth, and induce apoptosis [90]. The MTT test is really a sensitive

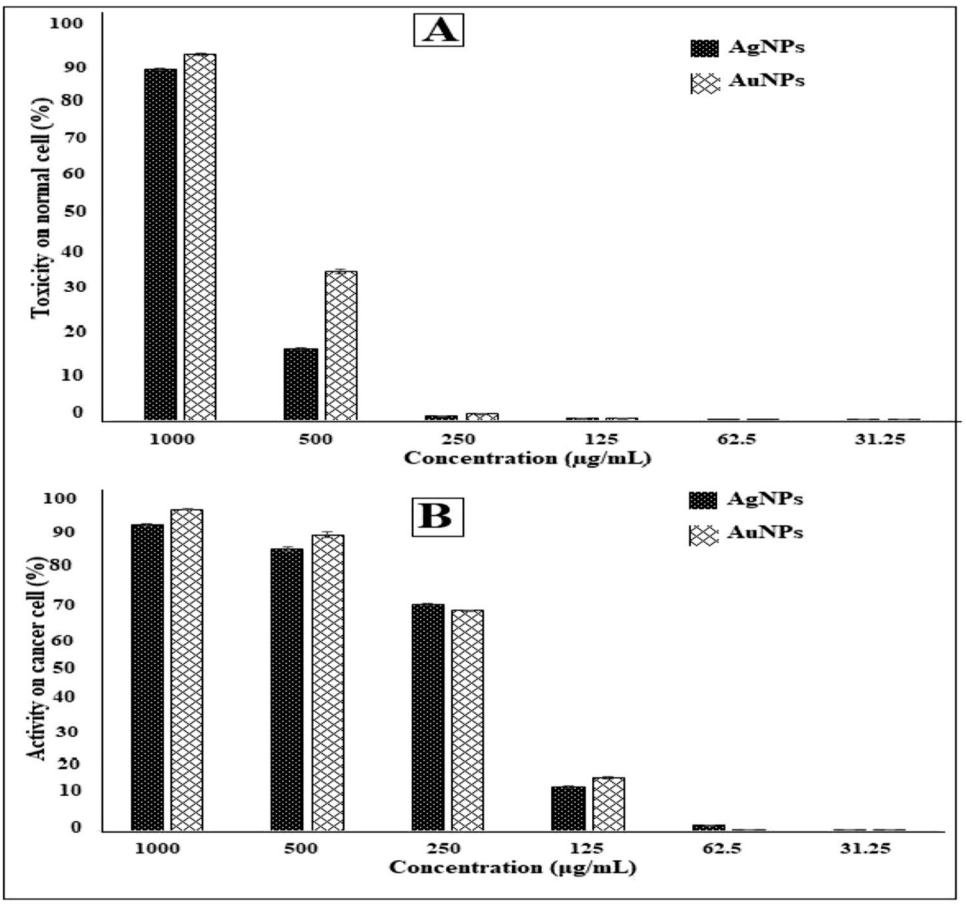

Fig. 12 Cytotoxicity (**A**) and antitumor activity (**B**) of AgNPs and AuNPs

colorimetric technique measuring determining the total number of viabilities in cell multiplication and cytotoxic activity experiments. Moreover, Fig. 12 shows cell death including both healthy and malignant cells significantly dose-dependent also when subjected to various quantities of either AgNPs or AuNPs. In specifically, our IC_{50} of Vero cell was 695.34 µg/mL for AgNPs and 631.66 µg/mL for AuNPs. AgNPs' IC_{50} for cancer cell (Mcf7) was 204.07 µg/mL, whereas AuNPs' IC_{50} was 206.95 µg/mL. In particular to maintain the protection of humans, it is thus strongly advised that the therapy with AgNPs and AuNPs be carried out at concentrations lower than 695.34 µg/mL and 631.66 µg/mL, respectively. Employing unique and diverse malignant cells, different studies have thoroughly investigated the cytotoxic effects of AgNPs as well as AuNPs [91, 92]. A parallel recent study showed that AgNPs and AuNPs had an antitumor impact on carcinoma cell lines. AgNPs and AuNPs were reported to have IC_{50} values of 100 and 200 µg/mL, respectively [92]. As a result, our investigation demonstrated more toxicity on carcinoma cell lines compared to the earlier findings [91, 92]. Applying AuNPs for medical purposes, Hamed as well as some co-workers showed anticancer properties versus carcinoma cell lines [93].

3.7 Antioxidant activity

Antioxidants are effective against reactive oxygen species (ROS), byproducts of biological activities [94]. Free radicals, which cause a range of diseases, may also be reduced by antioxidants [95]. Antioxidants were already considered as bioactive molecules provided; they show anticancer, antibacterial, anti-inflammatory, anti-mutagenic, anti-tumor, and anti-carcinogenic and properties. As shown in Fig. 13, the antioxidant activity of AgNPs and AuNPs was evaluated in this study using DPPH methods at a range of doses (1000–15.62 µg/mL). Results revealed that AgNPs had the strongest antioxidant activity comparing to AuNPs. AgNPs had an IC_{50} of 38.2 µg/mL as opposed to 180 µg/mL AuNPs. According to Pu et al., spherical AuNPs have stronger antioxidant potential than irregularly or polygonal ones [96]. In previous research, AgNPs showed strong DPPH efficacy with just an IC_{50} value of 30.04 µg/mL [97]. Our results confirm the outstanding antioxidant properties of AgNPs and AuNPs that have been previously described [98, 99].

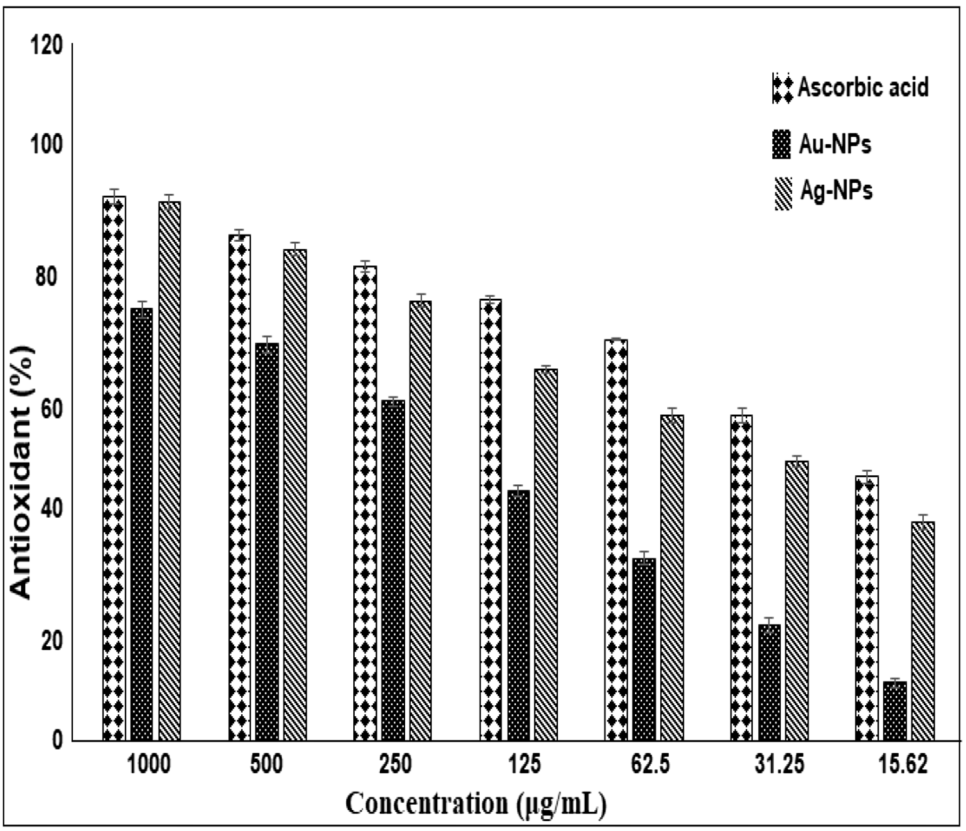

Fig. 13 Antioxidant activity of AgNPs and AuNPs by DPPH method

4 Conclusion

The novel fungus *Fusarium pseudonygamai* is used in the present discovery to synthesize AgNPs and AuNPs, which is a very effective and environmentally beneficial process. The generation of AgNPs and AuNPs with sizes between 5–20 nm for AgNPs and 8–60 nm for AuNPs was mediated by *Fusarium pseudonygamai* filtrate. Different analytical methods were used to analyze the produced AgNPs and AuNPs, and they were discovered that the particles were extremely stable. Effective antibacterial, antibiofilm, antioxidant, and anticancer properties have been demonstrated by the biosynthesized AgNPs and AuNPs. On Mcf7 cells, these AgNPs and AuNPs had strong cytotoxic properties. In the world of medical biotechnology, this alternative biosynthesis process for AgNPs and AuNPs would compete with the widely used chemical approaches.

Author contribution Conceptualization: Mohamed K. Y. Soliman, Mohammed Abu-Elghait, Salem S. Salem, and Mohamed Salah Azab; methodology and resources: Mohamed K.Y. Soliman, Mohammed Abu-Elghait, and Salem S. Salem; validation and visualization: Mohamed K.Y. Soliman, Mohammed Abu-Elghait, Salem S. Salem, and Mohamed Salah Azab; formal analysis: Mohamed K.Y. Soliman, Mohammed Abu-Elghait, Salem S. Salem, and Mohamed Salah Azab; writing—original draft preparation: Mohamed K.Y. Soliman, Mohammed Abu-Elghait, and Salem S. Salem; writing—review and editing: Mohamed K.Y. Soliman, Mohammed Abu-Elghait, Salem S. Salem, and Mohamed Salah Azab; supervision: Mohammed Abu-Elghait, Salem S. Salem, and Mohamed Salah Azab. All authors have read and agreed to the published version of the manuscript.

Funding Open access funding provided by The Science, Technology & Innovation Funding Authority (STDF) in cooperation with The Egyptian Knowledge Bank (EKB).

Data availability The data used to support the findings of this study are available from the corresponding author upon request.

Declarations

Ethics approval Not applicable.

Consent to participate Not applicable.

Consent for publication Not applicable.

Conflict of interest The authors declare no competing interests.

References

1. Salem SS, Fouda A (2021) Green synthesis of metallic nanoparticles and their prospective biotechnological applications: an overview. Biol Trace Elem Res 199(1):344–370. https://doi.org/10.1007/s12011-020-02138-3
2. Salem SS, Hammad EN, Mohamed AA, El-Dougdoug W (2023) A comprehensive review of nanomaterials: types, synthesis, characterization, and applications. Biointerface Res Appl Chem 13(1). https://doi.org/10.33263/BRIAC131.041
3. Al-Zahrani FAM, Salem SS, Al-Ghamdi HA, Nhari LM, Lin L, El-Shishtawy RM (2022) Green synthesis and antibacterial activity of Ag/Fe2O3 nanocomposite using Buddleja lindleyana extract. Bioengineering 9(9). https://doi.org/10.3390/bioengineering9090452
4. Shaheen TI, Salem SS, Zaghloul S (2019) A new facile strategy for multifunctional textiles development through in situ deposition of SiO_2/TiO_2 nanosols hybrid. Ind Eng Chem Res 58(44):20203–20212. https://doi.org/10.1021/acs.iecr.9b04655
5. Al-Rajhi AMH, Salem SS, Alharbi AA, Abdelghany TM (2022) Ecofriendly synthesis of silver nanoparticles using Kei-apple (Dovyalis caffra) fruit and their efficacy against cancer cells and clinical pathogenic microorganisms. Arab J Chem 15(7). https://doi.org/10.1016/j.arabjc.2022.103927
6. Salem SS, Badawy MSEM, Al-Askar AA, Arishi AA, Elkady FM, Hashem AH (2022) Green biosynthesis of selenium nanoparticles using orange peel waste: characterization, antibacterial and antibiofilm activities against multidrug-resistant bacteria. Life 12(6). https://doi.org/10.3390/life12060893
7. Hashem AH, Khalil AMA, Reyad AM, Salem SS (2021) Biomedical applications of mycosynthesized selenium nanoparticles using Penicillium expansum ATTC 36200. Biol Trace Elem Res 199(10):3998–4008. https://doi.org/10.1007/s12011-020-02506-z
8. Salem SS, Hashem AH, Sallam AAM, Doghish AS, Al-Askar AA, Arishi AA, Shehabeldine AM (2022) Synthesis of silver nanocomposite based on carboxymethyl cellulose: antibacterial, antifungal and anticancer activities. Polymers 14(16). https://doi.org/10.3390/polym14163352
9. Fouda A, El-Din Hassan S, Salem SS, Shaheen TI (2018) In-Vitro cytotoxicity, antibacterial, and UV protection properties of the biosynthesized zinc oxide nanoparticles for medical textile applications. Microb Pathog 125:252–261. https://doi.org/10.1016/j.micpath.2018.09.030
10. Saied E, Salem SS, Al-Askar AA, Elkady FM, Arishi AA, Hashem AH (2022) Mycosynthesis of hematite (α-Fe2O3) nanoparticles using Aspergillus niger and their antimicrobial and photocatalytic activities. Bioengineering 9(8). https://doi.org/10.3390/bioengineering9080397
11. Badawy AA, Abdelfattah NAH, Salem SS, Awad MF, Fouda A (2021) Efficacy assessment of biosynthesized copper oxide nanoparticles (CuO-NPs) on stored grain insects and their impacts on morphological and physiological traits of wheat (Triticum aestivum L.) Plant. Biology 10(3). https://doi.org/10.3390/biology10030233
12. Eid AM, Fouda A, Niedbała G, Hassan SE-D, Salem SS, Abdo AM, Hetta HF, Shaheen TI (2020) Endophytic Streptomyces laurentii mediated green synthesis of Ag-NPs with antibacterial and anticancer properties for developing functional textile fabric properties. Antibiotics 9(10):641
13. Salem SS, El-Belely EF, Niedbała G, Alnoman MM, Hassan SE, Eid AM, Shaheen TI, Elkelish A, Fouda A (2020) Bactericidal and In-Vitro Cytotoxic Efficacy of Silver Nanoparticles (Ag-NPs) Fabricated by endophytic actinomycetes and their use as coating for the textile fabrics. Nanomaterials 10(10). https://doi.org/10.3390/nano10102082
14. Shaheen TI, Fouda A, Salem SS (2021) Integration of cotton fabrics with biosynthesized CuO nanoparticles for bactericidal activity in the terms of their cytotoxicity assessment. Ind Eng Chem Res 60(4):1553–1563. https://doi.org/10.1021/acs.iecr.0c04880
15. Hammami I, AlabdallahJomaa NMAA, Kamoun M (2021) Gold nanoparticles: synthesis properties and applications. J King Saud Univ-Sci 33(7):101560. https://doi.org/10.1016/j.jksus.2021.101560
16. Guilger-Casagrande M, Lima RD (2019) Synthesis of silver nanoparticles mediated by fungi: a review. Front Bioeng Biotech 7.https://doi.org/10.3389/fbioe.2019.00287
17. Doghish AS, Hashem AH, Shehabeldine AM, Sallam A-AM, El-Sayyad GS, Salem SS (2022) Nanocomposite based on gold nanoparticles and carboxymethyl cellulose: synthesis, characterization, antimicrobial, and anticancer activities. J Drug Deliv Sci Technol 77:103874. https://doi.org/10.1016/j.jddst.2022.103874
18. Salem SS, Fouda MMG, Fouda A, Awad MA, Al-Olayan EM, Allam AA, Shaheen TI (2021) Antibacterial, cytotoxicity and larvicidal activity of green synthesized selenium nanoparticles using Penicillium corylophilum. J Cluster Sci 32(2):351–361. https://doi.org/10.1007/s10876-020-01794-8
19. Hashem AH, Shehabeldine AM, Ali OM, Salem SS (2022) Synthesis of chitosan-based gold nanoparticles: antimicrobial and wound-healing activities. Polymers 14(11). https://doi.org/10.3390/polym14112293
20. Sharaf MH, Nagiub AM, Salem SS, Kalaba MH, El Fakharany EM, Abd El-Wahab H (2022) A new strategy to integrate silver nanowires with waterborne coating to improve their antimicrobial and antiviral properties. Pigm Resin Technol. https://doi.org/10.1108/PRT-12-2021-0146
21. Abdelmoneim HEM, Wassel MA, Elfeky AS, Bendary SH, Awad MA, Salem SS, Mahmoud SA (2022) Multiple applications of CdS/TiO2 nanocomposites synthesized via microwave-assisted sol–gel. J Cluster Sci 33(3):1119–1128. https://doi.org/10.1007/s10876-021-02041-4
22. Hashem AH, Salem SS (2022) Green and ecofriendly biosynthesis of selenium nanoparticles using Urtica dioica (stinging nettle) leaf extract: antimicrobial and anticancer activity. Biotech J 17(2). https://doi.org/10.1002/biot.202100432
23. Abdelaziz AM, Salem SS, Khalil AMA, El-Wakil DA, Fouda HM, Hashem AH (2022) Potential of biosynthesized zinc oxide nanoparticles to control Fusarium wilt disease in eggplant (Solanum melongena) and promote plant growth. Biometals 35(3):601–616. https://doi.org/10.1007/s10534-022-00391-8
24. Salem SS (2022) Bio-fabrication of selenium nanoparticles using Baker's yeast extract and its antimicrobial efficacy on food borne pathogens. Appl Biochem Biotechnol 194(5):1898–1910. https://doi.org/10.1007/s12010-022-03809-8
25. Hammad EN, Salem SS, Mohamed AA, El-Dougdoug W (2022) Environmental impacts of ecofriendly iron oxide nanoparticles on dyes removal and antibacterial activity. Appl Biochem Biotechnol. https://doi.org/10.1007/s12010-022-04105-1
26. Mohamed AA, Abu-Elghait M, Ahmed NE, Salem SS (2021) Correction to: Eco-friendly mycogenic synthesis of ZnO and CuO nanoparticles for in vitro antibacterial, antibiofilm and antifungal applications (Biological Trace Element Research, (2021), 199, 7, (2788–2799), https://doi.org/10.1007/s12011-020-02369-4).

Biol Trace Elem Res 199 (7):2800–2801. https://doi.org/10.1007/s12011-020-02391-6
27. Al-Zahrani FAM, Al-Zahrani NA, Al-Ghamdi SN, Lin L, Salem SS, El-Shishtawy RM (2022) Synthesis of Ag/Fe2O3 nanocomposite from essential oil of ginger via green method and its bactericidal activity. Biomass Convers Biorefinery. https://doi.org/10.1007/s13399-022-03248-9
28. Hashem AH, Selim TA, Alruhaili MH, Selim S, Alkhalifah DHM, Al Jaouni SK, Salem SS (2022) Unveiling antimicrobial and insecticidal activities of biosynthesized selenium nanoparticles using prickly pear peel waste. J Funct Biomater 13(3). https://doi.org/10.3390/jfb13030112
29. Hammad EN, Salem SS, Zohair MM, Mohamed AA, El-Dougdoug W (2022) Purpureocillium lilacinum mediated biosynthesis copper oxide nanoparticles with promising removal of dyes. Biointerface Res Appl Chem 12(2):1397–1404. https://doi.org/10.33263/BRIAC122.13971404
30. Saied E, Eid AM, Hassan SED, Salem SS, Radwan AA, Halawa M, Saleh FM, Saad HA, Saied EM, Fouda A (2021) The catalytic activity of biosynthesized magnesium oxide nanoparticles (Mgo-nps) for inhibiting the growth of pathogenic microbes, tanning effluent treatment, and chromium ion removal. Catalysts 11(7). https://doi.org/10.3390/catal11070821
31. Abu-Elghait M, Hasanin M, Hashem AH, Salem SS (2021) Eco-friendly novel synthesis of tertiary composite based on cellulose and myco-synthesized selenium nanoparticles: Characterization, antibiofilm and biocompatibility. Int J Biol Macromol 175:294–303. https://doi.org/10.1016/j.ijbiomac.2021.02.040
32. Qureshi A, Blaisi NI, Abbas AA, Khan NA, Rehman S (2021) Prospectus and development of microbes mediated synthesis of nanoparticles. In: Microbial nanotechnology: green synthesis and applications. Springer, 1–15
33. Abdelghany TM, Al-Rajhi AMH, Yahya R, Bakri MM, Al Abboud MA, Yahya R, Qanash H, Bazaid AS, Salem SS (2022) Phyto-fabrication of zinc oxide nanoparticles with advanced characterization and its antioxidant, anticancer, and antimicrobial activity against pathogenic microorganisms. Biomass Conv Bioref. https://doi.org/10.1007/s13399-022-03412-1
34. Shaheen TI, Salem SS, Fouda A (2021) Current advances in fungal nanobiotechnology: mycofabrication and applications. In: Lateef A, Gueguim-Kana EB, Dasgupta N, Ranjan S (eds) Microbial nanobiotechnology: principles and applications. Springer Singapore, Singapore, 113–143. https://doi.org/10.1007/978-981-33-4777-9_4
35. Shehabeldine AM, Amin BH, Hagras FA, Ramadan AA, Kamel MR, Ahmed MA, Atia KH, Salem SS (2022) Potential antimicrobial and antibiofilm properties of copper oxide nanoparticles: time-kill kinetic essay and ultrastructure of pathogenic bacterial cells. Appl Biochem Biotechnol. https://doi.org/10.1007/s12010-022-04120-2
36. Salem SS (2022) Baker's yeast-mediated silver nanoparticles: characterisation and antimicrobial biogenic tool for suppressing pathogenic microbes. BioNanoScience. https://doi.org/10.1007/s12668-022-01026-5
37. Gade A, Gaikwad S, Duran N, Rai M (2014) Green synthesis of silver nanoparticles by Phoma glomerata. Micron 59:52–59. https://doi.org/10.1016/j.micron.2013.12.005
38. Soliman MKY, Salem SS, Abu-Elghait M, Azab MS (2022) Biosynthesis of silver and gold nanoparticles and their efficacy towards antibacterial, antibiofilm, cytotoxicity, and antioxidant activities. Appl Biochem Biotechnol. https://doi.org/10.1007/s12010-022-04199-7
39. El Domany EB, Essam TM, Ahmed AE, Farghali AA (2018) Biosynthesis physico-chemical optimization of gold nanoparticles as anti-cancer and synergetic antimicrobial activity using Pleurotus ostreatus fungus. J J Appl Pharm Sci 8(5):119–128
40. Elamawi RM, Al-Harbi RE, Hendi AA (2018) Biosynthesis and characterization of silver nanoparticles using Trichoderma longibrachiatum and their effect on phytopathogenic fungi. Egypt J Biol Pest Control 28(1):28. https://doi.org/10.1186/s41938-018-0028-1
41. Ahmad A, Mukherjee P, Senapati S, Mandal D, Khan MI, Kumar R, Sastry M (2003) Extracellular biosynthesis of silver nanoparticles using the fungus Fusarium oxysporum. Colloids Surf, B 28(4):313–318. https://doi.org/10.1016/S0927-7765(02)00174-1
42. Gaikwad SC, Birla SS, Ingle AP, Gade AK, Marcato PD, Rai M, Duran N (2013) Screening of different Fusarium species to select potential species for the synthesis of silver nanoparticles. J Braz Chem Soc 24:1974–1982
43. Kathiresan K, Manivannan S, Nabeel MA, Dhivya B (2009) Studies on silver nanoparticles synthesized by a marine fungus, Penicillium fellutanum isolated from coastal mangrove sediment. Colloids Surf, B 71(1):133–137. https://doi.org/10.1016/j.colsurfb.2009.01.016
44. Metuku RP, Pabba S, Burra S, Hima Bindu NSVSSSL, Gudikandula K, Singara Charya MA (2014) Biosynthesis of silver nanoparticles from Schizophyllum radiatum HE 863742.1: their characterization and antimicrobial activity. 3 Biotech 4(3):227–234. https://doi.org/10.1007/s13205-013-0138-0
45. Shelar GB, Chavan AM (2014) Fungus-mediated biosynthesis of silver nanoparticles and its antibacterial activity. Arch App Sci Res 6:111–114
46. Mohmed AA, Fouda A, Elgamal MS, El-Din Hassan S, Shaheen TI, Salem SS (2017) Enhancing of cotton fabric antibacterial properties by silver nanoparticles synthesized by new egyptian strain fusarium keratoplasticum A1–3. Egypt J Chem 60:63–71. https://doi.org/10.21608/ejchem.2017.1626.1137
47. Thakker JN, Dalwadi P, Dhandhukia PC (2013) Biosynthesis of gold nanoparticles using Fusarium oxysporum f. sp. cubense JT1, a plant pathogenic fungus. Int Sch Res Not
48. Du L, Xian L, Feng J-X (2011) Rapid extra-/intracellular biosynthesis of gold nanoparticles by the fungus Penicillium sp. J Nanopart Res 13(3):921–930. https://doi.org/10.1007/s11051-010-0165-2
49. Vala AK (2015) Exploration on green synthesis of gold nanoparticles by a marine-derived fungus Aspergillus sydowii. Environ Progress Sustain Energy 34(1):194–197
50. Jones KE, Patel NG, Levy MA, Storeygard A, Balk D, Gittleman JL, Daszak P (2008) Global trends in emerging infectious diseases. Nature 451(7181):990–993
51. Khan ST, Musarrat J, Al-Khedhairy AA (2016) Countering drug resistance, infectious diseases, and sepsis using metal and metal oxides nanoparticles: current status. Colloids Surf, B 146:70–83. https://doi.org/10.1016/j.colsurfb.2016.05.046
52. Elakraa AA, Salem SS, El-Sayyad GS, Attia MS (2022) Cefotaxime incorporated bimetallic silver-selenium nanoparticles: promising antimicrobial synergism, antibiofilm activity, and bacterial membrane leakage reaction mechanism. RSC Adv 12(41):26603–26619. https://doi.org/10.1039/D2RA04717A
53. Al-Dhabi NA, Mohammed Ghilan A-K, Arasu MV (2018) Characterization of silver nanomaterials derived from marine streptomyces sp. Al-Dhabi-87 and its in vitro application against multidrug resistant and extended-spectrum beta-lactamase clinical pathogens. Nanomaterials 8(5). https://doi.org/10.3390/nano8050279
54. Spagnoletti FN, Spedalieri C, Kronberg F, Giacometti R (2019) Extracellular biosynthesis of bactericidal Ag/AgCl nanoparticles for crop protection using the fungus Macrophomina phaseolina. J Environ Manage 231:457–466. https://doi.org/10.1016/j.jenvman.2018.10.081
55. Razavi R, Molaei R, Moradi M, Tajik H, Ezati P, Shafipour Yordshahi A (2020) Biosynthesis of metallic nanoparticles using mulberry fruit (Morus alba L) extract for the preparation of

antimicrobial nanocellulose film. Appl Nanosci 10(2):465–476. https://doi.org/10.1007/s13204-019-01137-8
56. Girón-Vázquez NG, Gómez-Gutiérrez CM, Soto-Robles CA, Nava O, Lugo-Medina E, Castrejón-Sánchez VH, Vilchis-Nestor AR, Luque PA (2019) Study of the effect of Persea americana seed in the green synthesis of silver nanoparticles and their antimicrobial properties. Results Phys 13:102142. https://doi.org/10.1016/j.rinp.2019.02.078
57. Yousef A, Abu-Elghait M, Barghoth MG, Elazzazy AM, Desouky SE (2022) Fighting multidrug-resistant *Enterococcus faecalis* via interfering with virulence factors using green synthesized nanoparticles. Microb Pathog 173:105842. https://doi.org/10.1016/j.micpath.2022.105842
58. Roy R, Tiwari M, Donelli G, Tiwari V (2018) Strategies for combating bacterial biofilms: a focus on anti-biofilm agents and their mechanisms of action. Virulence 9(1):522–554. https://doi.org/10.1080/21505594.2017.1313372
59. Ibrahim SA, Fayed EA, Rizk HF, Desouky SE, Ragab A (2021) Hydrazonoyl bromide precursors as DHFR inhibitors for the synthesis of bis-thiazolyl pyrazole derivatives; antimicrobial activities, antibiofilm, and drug combination studies against MRSA. Bioorg Chem 116:105339
60. Nassar O, Desouky SE, El-Sherbiny GM, Abu-Elghait M (2022) Correlation between phenotypic virulence traits and antibiotic resistance in *Pseudomonas aeruginosa* clinical isolates. Microb Pathog 162:105339. https://doi.org/10.1016/j.micpath.2021.105339
61. Vickers NJ (2017) Animal communication: when I'm calling you, will you answer too? Curr Biol 27(14):R713–R715
62. Waters EM, Rowe SE, O'Gara JP, Conlon BPJPp (2016) Convergence of Staphylococcus aureus persister and biofilm research: can biofilms be defined as communities of adherent persister cells? 12(12):e1006012
63. Huh AJ, Kwon YJ (2011) "Nanoantibiotics": a new paradigm for treating infectious diseases using nanomaterials in the antibiotics resistant era. J Control Release : Off J Control Release Soc 156(2):128–145. https://doi.org/10.1016/j.jconrel.2011.07.002
64. Javanbakht T, Ghane-Motlagh B, Sawan M (2020) Comparative study of antibiofilm activity and physicochemical properties of microelectrode arrays. Microelectron Eng 229:111305. https://doi.org/10.1016/j.mee.2020.111305
65. Salama Y, Chennaoui M, Sylla A, Mountadar M, Rihani M, Assobhei O (2016) Characterization, structure, and function of extracellular polymeric substances (EPS) of microbial biofilm in biological wastewater treatment systems: a review. Desalin Water Treat 57(35):16220–16237
66. Hentzer M, Teitzel GM, Balzer GJ, Heydorn A, Molin S, Givskov M, Parsek MR (2001) Alginate overproduction affects Pseudomonas aeruginosa biofilm structure and function. J Bacteriol 183(18):5395–5401
67. Wijkmans JCHM, Beckett RP (2002) Combinatorial chemistry in anti-infectives research. Drug Discovery Today 7:126–132. https://doi.org/10.1016/S1359-6446(02)00007-7
68. Shehabeldine AM, Salem SS, Ali OM, Abd-Elsalam KA, Elkady FM, Hashem AH (2022) Multifunctional silver nanoparticles based on chitosan: antibacterial, antibiofilm, antifungal, antioxidant, and wound-healing activities. J Fungi 8(6):612
69. Lafon-Hughes L, Di Tomaso MV, Méndez-Acuña L, Martínez-López W (2008) Chromatin-remodelling mechanisms in cancer. Mutat Res/Rev Mutat Res 658(3):191–214. https://doi.org/10.1016/j.mrrev.2008.01.008
70. Wang Y, Sun S, Zhang Z, Shi D (2018) Nanomaterials for cancer precision medicine. Adv Mater 30(17):1705660
71. Hamed A, Abdel-Razek AS, Araby M, Abu-Elghait M, El-Hosari DG, Frese M, Soliman HS, Stammler HG, Sewald N, Shaaban M (2021) Meleagrin from marine fungus Emericella dentata Nq45: crystal structure and diverse biological activity studies. Nat Prod Res 35(21):3830–3838
72. Salem SS, Ali OM, Reyad AM, Abd-Elsalam KA, Hashem AH (2022) Pseudomonas indica-mediated silver nanoparticles: antifungal and antioxidant biogenic tool for suppressing Mucormycosis fungi. J Fungi 8(2):126
73. Philip S, Kundu GC (2003) Osteopontin induces nuclear factor κB-mediated promatrix metalloproteinase-2 activation through IκBα/IKK signaling pathways, and curcumin (diferulolylmethane) down-regulates these pathways. J Biol Chem 278(16):14487–14497
74. Pourali P, Yahyaei B, Afsharnezhad S (2018) Bio-synthesis of gold nanoparticles by Fusarium oxysporum and assessment of their conjugation possibility with two types of β-lactam antibiotics without any additional linkers. Microbiology 87(2):229–237. https://doi.org/10.1134/S0026261718020108
75. Rashid MI, Mujawar LH, Rehan ZA, Qari H, Zeb J, Almeelbi T, Ismail IMI (2016) One-step synthesis of silver nanoparticles using Phoenix dactylifera leaves extract and their enhanced bactericidal activity. J Mol Liq 223:1114–1122. https://doi.org/10.1016/j.molliq.2016.09.030
76. Patil MP, Ngabire D, Thi HHP, Kim M-D, Kim G-D (2017) Eco-friendly synthesis of gold nanoparticles and evaluation of their cytotoxic activity on cancer cells. J Cluster Sci 28(1):119–132. https://doi.org/10.1007/s10876-016-1051-6
77. Horstmann Risso N, Ottonelli Stopiglia CD, Oliveira MT, Haas SE, Ramos Maciel T, Reginatto Lazzari N, Kelmer EL, Pinto Vilela JA, Beckmann DV (2020) Chlorhexidine nanoemulsion: a new antiseptic formulation. Int J Nanomed 15:6935–6944. https://doi.org/10.2147/ijn.S228280
78. Elbahnasawy MA, Shehabeldine AM, Khattab AM, Amin BH, Hashem AH (2021) Green biosynthesis of silver nanoparticles using novel endophytic Rothia endophytica: Characterization and anticandidal activity. J Drug Deliv Sci Technol 62:102401. https://doi.org/10.1016/j.jddst.2021.102401
79. Naimi-Shamel N, Pourali P, Dolatabadi S (2019) Green synthesis of gold nanoparticles using Fusarium oxysporum and antibacterial activity of its tetracycline conjugant. J de Mycologie Médicale 29(1):7–13. https://doi.org/10.1016/j.mycmed.2019.01.005
80. Vivek R, Thangam R, Muthuchelian K, Gunasekaran P, Kaveri K, Kannan S (2012) Green biosynthesis of silver nanoparticles from Annona squamosa leaf extract and its in vitro cytotoxic effect on MCF-7 cells. Process Biochem 47(12):2405–2410. https://doi.org/10.1016/j.procbio.2012.09.025
81. Alsharif SM, Salem SS, Abdel-Rahman MA, Fouda A, Eid AM, El-Din Hassan S, Awad MA, Mohamed AA (2020) Multifunctional properties of spherical silver nanoparticles fabricated by different microbial taxa. Heliyon 6(5):e03943. https://doi.org/10.1016/j.heliyon.2020.e03943
82. Gopinath K, Arumugam A (2014) Extracellular mycosynthesis of gold nanoparticles using Fusarium solani. Appl Nanosci 4(6):657–662. https://doi.org/10.1007/s13204-013-0247-4
83. Dinesh S, Karthikeyan S, Arumugam P (2012) Biosynthesis of silver nanoparticles from Glycyrrhiza glabra root extract. Arch Appl Sci Res 4(1):178–187
84. Velázquez-Velázquez JL, Santos-Flores A, Araujo-Meléndez J, Sánchez-Sánchez R, Velasquillo C, González C, Martínez-Castañon G, Martinez-Gutierrez F (2015) Anti-biofilm and cytotoxicity activity of impregnated dressings with silver nanoparticles. Mater Sci Eng, C 49:604–611
85. Joshi AS, Singh P, Mijakovic I (2020) Interactions of gold and silver nanoparticles with bacterial biofilms: Molecular interactions behind inhibition and resistance. Int J Mol Sci 21(20):7658
86. Aref MS, Salem SS (2020) Bio-callus synthesis of silver nanoparticles, characterization, and antibacterial activities via

Cinnamomum camphora callus culture. Biocatal Agric Biotechnol 27:101689. https://doi.org/10.1016/j.bcab.2020.101689
87. Rajkumari J, Busi S, Vasu AC, Reddy P (2017) Facile green synthesis of baicalein fabricated gold nanoparticles and their antibiofilm activity against Pseudomonas aeruginosa PAO1. Microb Pathog 107:261–269. https://doi.org/10.1016/j.micpath.2017.03.044
88. Khan F, Manivasagan P, Lee J-W, Pham DT, Oh J, Kim Y-M (2019) Fucoidan-stabilized gold nanoparticle-mediated biofilm inhibition, attenuation of virulence and motility properties in Pseudomonas aeruginosa PAO1. Marine Drugs 17(4). https://doi.org/10.3390/md17040208
89. Estevez MB, Raffaelli S, Mitchell SG, Faccio R, Alborés S (2020) Biofilm eradication using biogenic silver nanoparticles. Molecules 25(9):2023
90. Popescu R, Heiss EH, Ferk F, Peschel A, Knasmueller S, Dirsch VM, Krupitza G, Kopp B (2011) Ikarugamycin induces DNA damage, intracellular calcium increase, p38 MAP kinase activation and apoptosis in HL-60 human promyelocytic leukemia cells. Mutat Res/Fundam Mol Mech Mutagen 709:60–66
91. Krishnaraj C, Muthukumaran P, Ramachandran R, Balakumaran M, Kalaichelvan P (2014) Acalypha indica Linn: biogenic synthesis of silver and gold nanoparticles and their cytotoxic effects against MDA-MB-231, human breast cancer cells. Biotech Rep 4:42–49
92. Kuppusamy P, Ichwan SJ, Al-Zikri PNH, Suriyah WH, Soundharrajan I, Govindan N, Maniam GP, Yusoff MM (2016) In vitro anticancer activity of Au, Ag nanoparticles synthesized using Commelina nudiflora L. aqueous extract against HCT-116 colon cancer cells. Biol Trace Elem Res 173(2):297–305
93. Hamed MM, Abdelftah LS (2019) Biosynthesis of gold nanoparticles using marine Streptomyces griseus isolate (M8) and evaluating its antimicrobial and anticancer activity. Egypt J Aquat Biol Fish 23(1):173–184
94. Kurutas EB (2015) The importance of antioxidants which play the role in cellular response against oxidative/nitrosative stress: current state. Nutr J 15(1):1–22
95. Pham-Huy LA, He H, Pham-Huy C (2008) Free radicals, antioxidants in disease and health. Int J Biomed Sci: IJBS 4(2):89
96. Pu S, Li J, Sun L, Zhong L, Ma Q (2019) An in vitro comparison of the antioxidant activities of chitosan and green synthesized gold nanoparticles. Carbohyd Polym 211:161–172. https://doi.org/10.1016/j.carbpol.2019.02.007
97. Mohanta YK, Panda SK, Jayabalan R, Sharma N, Bastia AK, Mohanta TK (2017) Antimicrobial, antioxidant and cytotoxic activity of silver nanoparticles synthesized by leaf extract of Erythrina suberosa (Roxb.). Front Mol Biosci 4:14
98. Dipankar C, Murugan S (2012) The green synthesis, characterization and evaluation of the biological activities of silver nanoparticles synthesized from Iresine herbstii leaf aqueous extracts. Colloids Surf, B 98:112–119. https://doi.org/10.1016/j.colsurfb.2012.04.006
99. Sathishkumar G, Jha PK, Vignesh V, Rajkuberan C, Jeyaraj M, Selvakumar M, Jha R, Sivaramakrishnan SJJoML (2016) Cannonball fruit (Couroupita guianensis, Aubl.) extract mediated synthesis of gold nanoparticles and evaluation of its antioxidant activity. 215:229–236